

1 **Supplementary information**

2 **Facile mass preparation and characterization of Al/copper ferrites**  
3 **metastable intermolecular energetic nanocomposites**

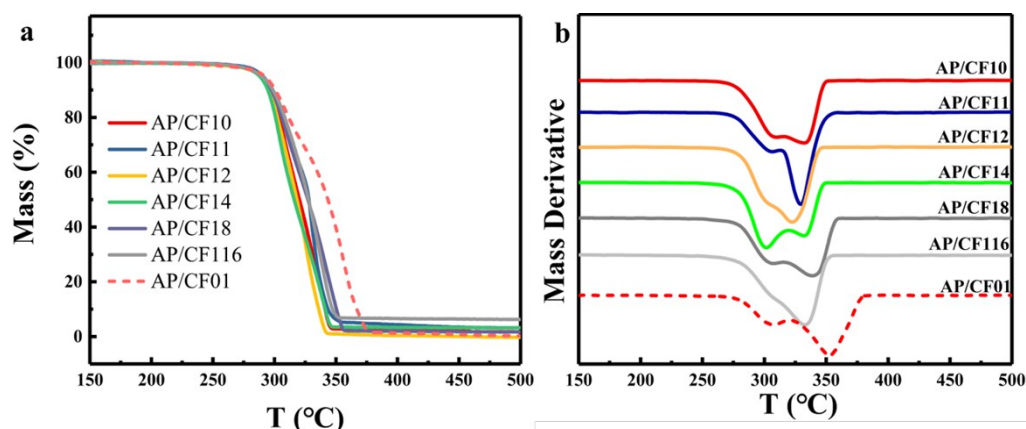
4 Chao Sang<sup>a, b</sup>, Keke Chen<sup>a, b</sup>, Guoping Li<sup>a, b, \*</sup>, Shaohua Jin<sup>a, b</sup>, Yunjun Luo<sup>a, b, \*</sup>

5 a. School of Materials Science and Engineering Technology, Beijing Institute of Technology, Beijing  
6 100081;

7 b. Key Laboratory for Ministry of Education of High Energy Density Materials, Beijing 100081

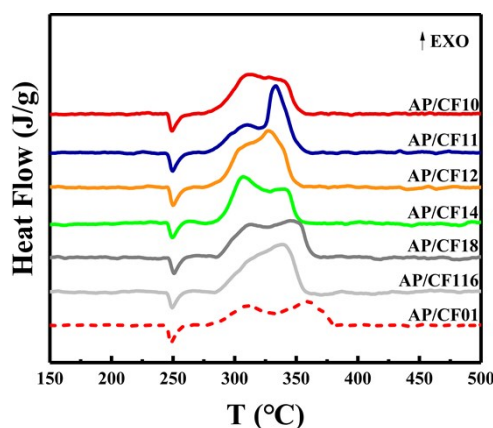
8 \*Corresponding author. E-mail: [girlping3114@bit.edu.cn](mailto:girlping3114@bit.edu.cn), [yjluo@bit.edu.cn](mailto:yjluo@bit.edu.cn)

9



10

11 **Figure S1. TG (a) and DTG (b) curves of AP/copper ferrites.**



12

13 **Figure S2. DSC curves of AP/copper ferrites.**

14 CF10, CF11, CF12, CF14, CF18, CF116, CF01 respectively refer to the copper ferrites with molar

15 ratio of Cu and Fe in the raw materials of 1:0, 1:1, 1:2, 1:4, 1:8, 1:16 and 0: 1. AP/CF\*\* is the

16 mixture of AP and copper ferrites. AP/CF14 shows the lowest  $T_{Lmax}$  and  $T_{LEXO}$ , and the highest

17 weight loss ratio and heat release ratio at the LTD stage, indicating that CF14 has the highest

18 catalytic activity for the LTD of AP. The overall catalytic activities of the copper ferrites for the LTD

19 of AP are in the order of CF14 > CF12 > CF11 > CF18 > CF116 > CF01 > CF10. Similarly,

20 AP/CF12 shows the highest catalytic activity for the HTD of AP with the lowest  $T_{Hmax}$  and  $T_{HEXO}$ ,

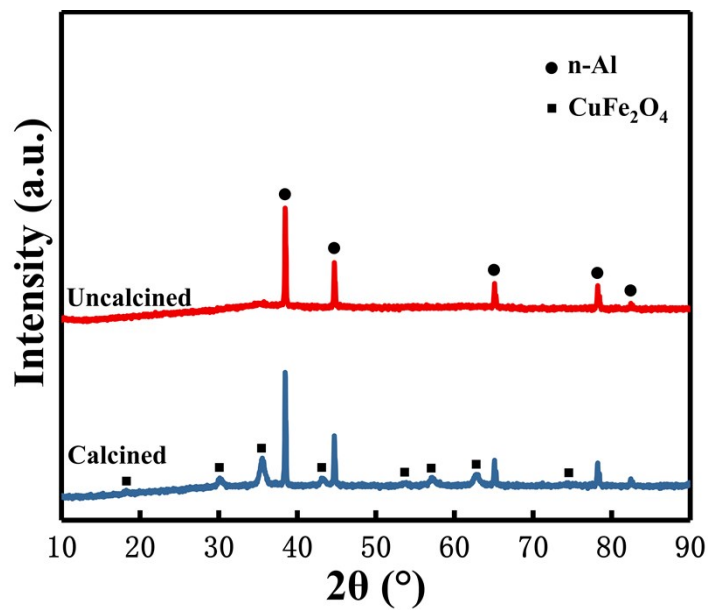
21 and the catalytic activities of the copper ferrites for the HTD of AP follow the order of CF12 > CF11 >

22 CF14 > CF10 > CF116 > CF18 > CF01. The  $T_{Hmax}$  of AP/CF11, AP/CF14, and AP/CF10 are very

23 close to each other. Based on these results, it can be concluded that CF14 possess the highest

24 catalytic activities for the thermal decomposition of AP.

25



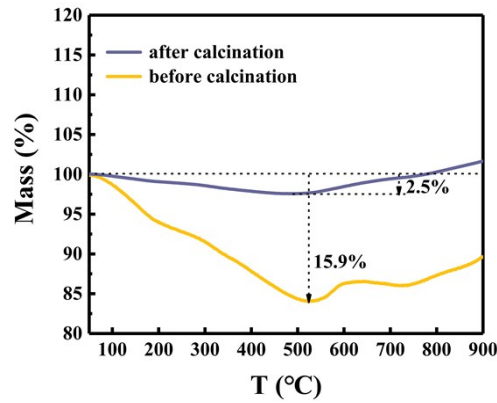
27

28 **Figure S3. X-ray diffraction patterns of CFA3 before and after calcination.**

29 It shows the crystal forms before and after calcination. Before calcination, only the diffraction  
30 peaks of Al were present. After calcination, the diffraction peaks of copper ferrites crystal form  
31 appeared but the diffraction peaks of Al did not change.

32

33



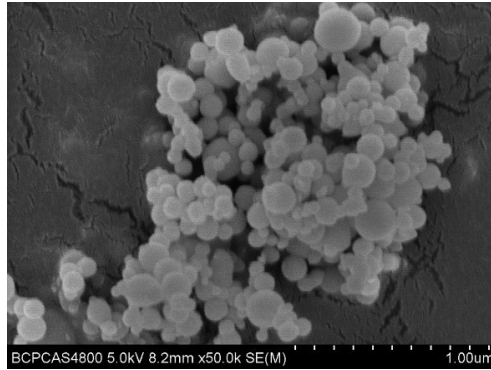
34

35 **Figure S4. TG curves of CFA3 before and after calcination.**

36 It shows the TG curves of CFA3 before and after calcination. The weight loss of the sample before  
37 calcination was as high as 15.9%, while it was only 2.5% after calcination. This shows that the  
38 impurities are basically removed after calcination, indicating that the calcination time and  
39 temperature used are feasible.

40

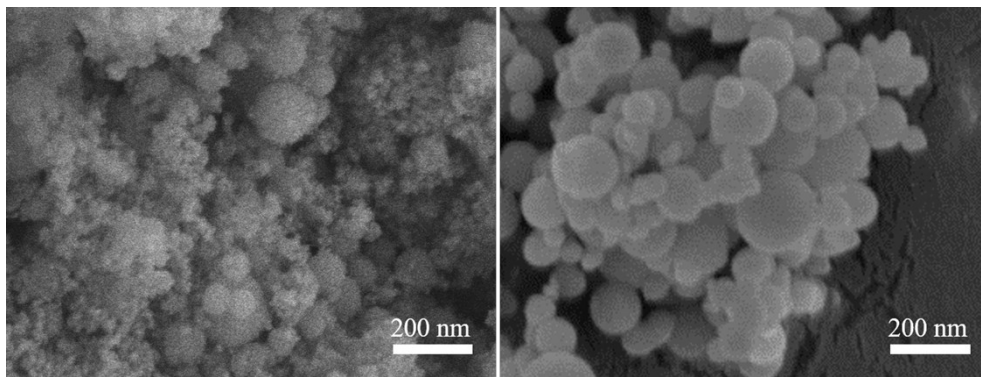
41



42

43 **Figure S5. SEM image of pure n-Al.**

44 It shows that n-Al is spherical, with an average particle size of about 90 nm and a wide particle  
45 size distribution. The spherical n-Al particles have a smooth surface.

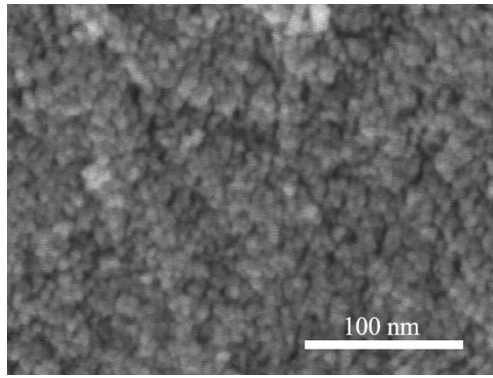


46

47 **Figure S6. Partially enlarged comparison image of Al/copper ferrites (CFA7, left) and n-Al**  
48 **(right).**

49 By comparison, it can be found that the n-Al surface in CFA7 is rougher than that of pure n-Al,  
50 which indicates that copper ferrites exist on the n-Al surface.

51

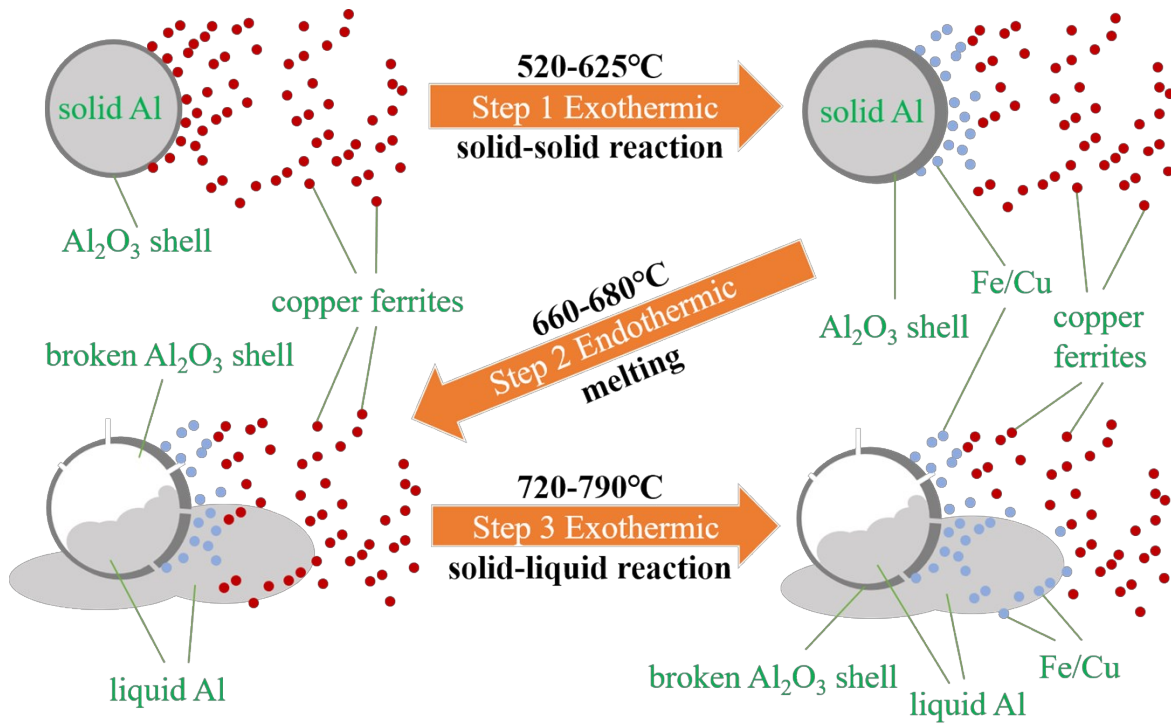


52

53 **Figure S7. SEM image of copper ferrites particles (CF14).**

54 It can be found that the bulk CF is composed of nano-sized particles.

55



56

57 **Figure S8. Schematic diagram of the thermite reaction process.**

58



60 **Table S1. Specific surface area data of CuO, Fe<sub>2</sub>O<sub>3</sub> and copper ferrites**

Sample	CuO (CF10)	copper ferrites (CF14)	Fe <sub>2</sub> O <sub>3</sub> (CF01)
S <sub>BET</sub> (cm <sup>2</sup> /g)	2.88	60.22	87.92